Photovoltaic Water Pumping Systems Based on Standard Components

Dionizio José Vargas Roman

Dissertation presented to the School of Technology and Management of Polytechnic
Institute of Bragança to the Fulfillment of the Requirements for the Master of Science
Degree in Industrial Engineering (Electrical Engineering branch), in the scope of Double
Degree with Federal University of Technology - Paraná

Supervised by:

Professor Ph.D. Américo Vicente Teixeira Leite

Professor Ph.D. Ângela Paula Barbosa de Silva Ferreira

Professor Ph.D. Alessandro Goedtel

This work does not include the appointments and suggestions of the Juri

Bragança

2018

Photovoltaic Water Pumping Systems Based on Standard Components

Dionizio José Vargas Roman

Dissertation presented to the School of Technology and Management of Polytechnic Institute of Bragança to the Fulfillment of the Requirements for the Master of Science Degree in Industrial Engineering (Electrical Engineering branch), in the scope of Double Degree with Federal University of Technology - Paraná.

Supervised by:

Professor Ph.D. Américo Vicente Teixeira Leite

Professor Ph.D. Ângela Paula Barbosa de Silva Ferreira

Professor Ph.D. Alessandro Goedtel

This work does not include the appointments and suggestions of the Juri

Bragança

2018

Dedication

To my beloved grandmother,

Érica Roman.

Acknowledgment

Abstract

The depletion of fossil fuels and their rising prices, increase researches in renewable energy sources. Furthermore, about 11.4% of global population (822 million people) lack basic drinking water service. Thus, photovoltaic water pumping systems (PVWPS) are an interesting solution to provide water in remote areas, which nowadays mostly of the systems are diesel based. PVWPS are commercially available as integrated sets of components, using a pump with a motor and a controller. Normally, small or very small companies are those who install these systems. They are dependent on the system itself and on the manufacturer. The only benefit of this companies comes from the installation they provide to the end user. Since they are not able to develop their own systems. This work presents different strategies for photovoltaic water pumping systems based on standard frequency converters, which are off-the-shelf and widely available, for different power levels. A new approach for low power applications is proposed, using only one or two photovoltaic modules, a centrifugal AC pump driven by a standard frequency converter. These approaches are valuable for small companies to develop their own cost-effective solutions.

Keywords: Photovoltaic Pumping, Frequency Converter, AC pump.

x

Resumo

O esgotamento de combustíveis fósseis e o aumento de seu preço, aumentaram as pesquisas sobre energias renováveis. Além disso, cerca de 11.4% da população global (822 milhões de pessoas) não tem acesso a serviços básicos de água potável. Assim, sistemas fotovoltaicos de bombagem de agua (PVWPS) são uma solução interessante para fornecer água em áreas remotas. PVWPS estão disponíveis comercialmente como um conjunto integrado de componentes, usando uma bomba acoplada a um motor e um controlador. Normalmente, são empresas pequenas ou muito pequenas que instalam estes sistemas. Elas são dependentes no sistema e nos fabricantes. O único benefício dessas empresas provem da instalação que eles realizam para o consumidor final. Como elas não são capazes de desenvolver seus próprios sistemas. Este trabalho apresenta diferentes estratégias para sistemas fotovoltaicos de bombagem de água baseados em inversores de frequência convencionais, que são componentes comuns e amplamente disponíveis, em diferentes níveis de potência. Uma nova abordagem para aplicações de baixa potência é proposta, usando somente um ou dos módulos fotovoltaicos, uma bomba AC centrífuga acionada por um inversor de frequência convencional. Essas abordagens são de grande valor para pequenas companhias desenvolverem suas próprias soluções economicamente viáveis.

Palavras-chave: Bombagem fotovoltaica, Inversor de frequência, Bomba AC.

Contents

List of Tables

List of Figures

Acronyms

ABB Asea Brown Baveri.

CCGT Combined Cycle Gas Turbine.

EU European Union.

LCOE Levelized Cost of Energy.

MPPT Maximum Power Point Tracking.

PID Proportional Integral Derivative.

PV Photovoltaic.

PVWPS Photovoltaic Water Pumping System.

RES Renewable Energy Sources.

SFC Standard Frequency Converter.

STC Standard Test Conditions.

VSD Variable Speed Drive.

WHO World Health Organization.

Symbols

ω_p Pump's speed.

$\mathbf{I}_{bat-in}$ Battery input current.

$\mathbf{I}_{bat-out}$ Battery output current.

$\mathbf{I}_{pv}$ Photovoltaic module current.

$\mathbf{I}_p$ Pump's current.

$\mathbf{K}_p$ Proportional gain.

$\mathbf{T}_d$ Derivative time.

$\mathbf{T}_i$ Integrative time.

$\mathbf{V}_{bat}$ Battery Voltage.

$\mathbf{V}_{DC}$ DC link voltage.

$\mathbf{V}_{mpp}$ Maximum power point voltage.

$\mathbf{V}_{oc}$ Open circuit voltage.

$\mathbf{V}_{Ref}$ Reference voltage.

Chapter 1

Introduction

According to the World Health Organization (WHO), in 2015, 844 million people still lacked even a basic drinking water service, defined as drinking water from an improved source, provided collection time is not more than 30 minutes for a round trip [1]. Furthermore, 663 million people (10% of world's population) still drank water from sources with little or no protection against contamination, being almost half of them from sub-Saharan Africa, which, eight in 10 live in rural areas [2].

The use of solar energy in water pumping systems is a key contribution to ensure energy for water supply and also environment preservation [3]. Solar Photovoltaic (PV) can minimize the dependence on diesel, gas or coal based electricity [4]. This green energy technology can play a major role as water is the key to agriculture. For this purpose, green affordable water pumping systems have much importance [3].

Still today, in agriculture, in developing countries, and in this region (Trás-os-Montes, Portugal), there are a lot of people who use water pump coupled with combustion engines. This still happens, because these places are distant from the electrical grid, and the Photovoltaic Water Pumping Systems (PVWPS) are little disseminated and expensive. This work contributes to solve this problem.

1.1   Problem Formulation

PVWPS are commercially available as integrated sets of components, using a pump with a motor, a controller and sensors. Commonly, small electrical installations companies are responsible for the most part of the installations of PVWPS. These are dependent on big companies' kits, which have the know-how to develop the components used. Regarding small companies, their only profit comes from the installation provided to the end user.

The first proposed PVWPS were DC pumps, waiving power conversion components between the PV modules and the load. However, DC pumps are more expensive and need more maintenance than AC pumps. Nowadays, AC kits are sold as closed solutions, using specific equipments from big manufacturers, utilizing dedicated Variable Speed Drive (VSD) or Standard Frequency Converters (SFC) to convert DC energy to AC, to supply an AC Pump. These energy converters are designed to be fed by the power grid and, therefore, they require a high DC-link voltage. This means that PV strings, which can be direct connected to frequency converter, need several modules to achieve such voltage levels. Power modules can be developed to solve these drawbacks [5], but this solution is still based on dedicated components, that small companies typically do not have the know-how to develop.

This handicap can be overcome developing innovative solutions, at cost-effective prices, based on standard components, such as frequency converters and AC water pumps, which are off-the-shelf equipment and widely available for industry applications. Actually, this challenge was proposed by the companies VALLED Soluções Energéticas and J.G. Instalações Elétricas, from Bragança - Portugal.

1.2   Objectives

This project intends to research the current PVWPS available in the market and to develop alternative and competitive systems, based on conventional components, namely for low power applications. Some objectives can be summarized as follows:

- Connect a PV module directly to a SFC, for low power applications.

- Use a low-cost and widely available power converter.

- Implement a solution to solve the lack of Maximum Power Point Tracking (MPPT) in SFC.

- Control the pump's speed according to the radiance level.

- Robust and reliable PVWPS.

- Implement a solution to solve the cases of instability due to a sudden fall of irradiance, lack of protections against empty well and full tank states.

In PVWPS for low power applications, up to 1.5 kW, other objectives can be added:

- Still use SFC, even with PV arrays low output voltages.

- Reduce the number of PV modules necessary to supply the load.

- Avoid batteries as energy storage components.

This work presents the solutions for PVWPS based on SFC for different power levels, and proposes a new approach for low power applications, using only one or two PV modules.

1.3 Document Structure

This dissertation is divided into six chapters, to describe the work developed during the research.

Chapter 1 presents an introduction to PVWPS in the current context, as well as the problem formulation.

A theoretical review of PV energy generation, the current state of the art of PVWPS, and the solutions based on SFC are presented in Chapter 2.

Chapter 3 presents the case studies of PVWPS and describes its challenges.

Chapter 4 presents a a new approach proposal for low power PVWPS, with a system description and explains how the pump's speed follows the irradiance level.

Chapter 5 contains the validation of the new approach proposal for low power PVWPS.

The final conclusions of ideas and suggestions for future works are presented in chapter 6.

Chapter 2

State of the Art

Nowadays, due to the increasing cost of electricity and exhaustion of fossil-based resources, there is a continuous growth of interest in renewable energy such as Solar, Wind, Biomass, and many others. Thus, due to attractive of Photovoltaic (PV) characteristics as low level of maintenance, high life expectancy and payback, PV systems are a viable alternative for energy generation, and stand-alone applications. There is a natural relation between the need for water pumping systems and availability of solar radiation [6]. When those two occurrences happen in remote areas, which are far from the grid, PV stand-alone systems are an interesting application for human consumption and crop irrigation. Photovoltaic Water Pumping System (PVWPS) have been a promising area of research during the last five decades. Nowadays, the utilization of PV energy to power water pumps is an emerging technology with great challenges [7].

This chapter presents an overview of the PV energy generation and market trends. Then, a summary of the current state of the art related to PVWPS is also presented. Finally, the advantages and drawbacks related to this kind of systems are discussed.

2.1 Photovoltaic Energy Generation

Energy generation based on fossil fuels still have the lead in the electric energy sector. However, their price volatility and considerable environmental impact encourage the

spread of Renewable Energy Sources (RES) in the global energy mix [8]. Thus, the energy sector is currently through a transition process. Nowadays, natural gas, the rapidly grown of renewable energies, and energy efficiency have taken the lead in new installations for energy generation. In European Union (EU), the market is also rapidly changing, with prospects for energy sector showing that RES can represent 80% of new capacity installations soon after 2030 [9]. In 2016, the solar PV generation market connected to the electrical grid was about 76.6 GW, which represents a growth of 50% compared to the 51.2 GW installed in 2015 [10].

The large development of PV systems is led by China and India, which may translate in the grow of these systems as the largest low-carbon generation source by 2040, and also substantial decrease in their costs. Currently, RES meet 40% of world energy needs, thus, marking the end for coal boom years [9]. Furthermore, the actual Levelized Cost of Energy (LCOE)[1], of utility-scale solar PV systems, shows that this energy conversion strategy is cheaper than Combined Cycle Gas Turbine (CCGT), coal and nuclear power plants, as presented in Figure 2.1 [12].
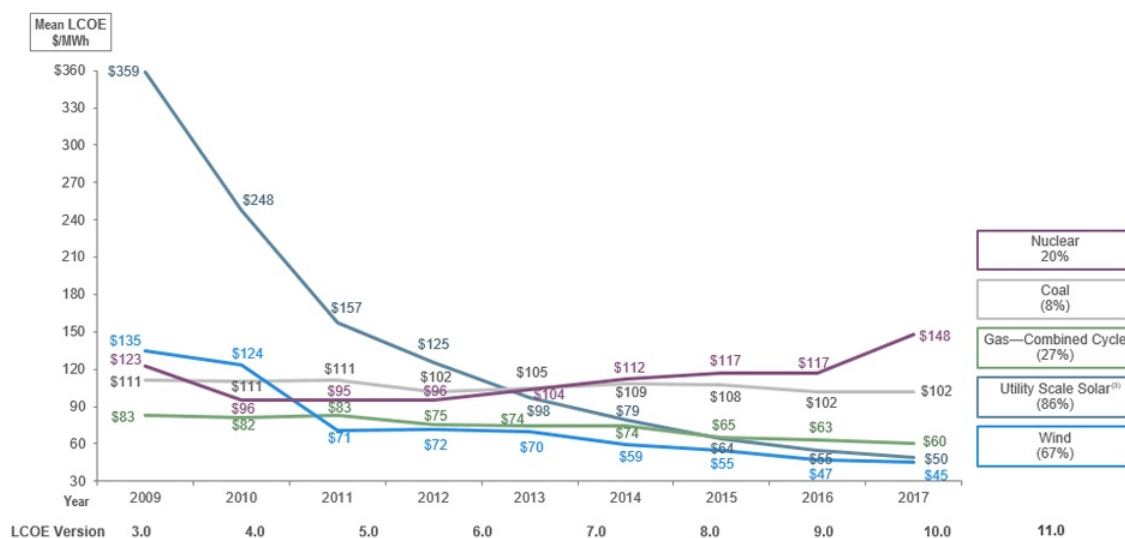
Figure 2.1: LCOE comparison of different energy sources. Adapted from [12].

---

[1]LCOE is a marketing tool used to compare the relative cost of energy produced by different energy-generating sources. It is evaluated by dividing lifetime by energy production [11].

2.2 Photovoltaic Water Pumping Systems

PVWPS are very important in remote, isolated, and non-electrified places, where the connection to the main grid is either difficult to establish or the cost is very high [4]. These systems are an alternative to conventional pumping systems - electricity and diesel based - and a cost effective application in remote off-grid areas of developing countries, and still in the developed ones. They are operate more effectively than other traditional water pumping systems [13].

This kind of system is integrates a PV module, a power control or conversion system, a motor coupled to a pump and some sensors. In Figure 2.2, is shown the structural outline of PVWPS. The basic component is the PV module which converts solar energy into electrical energy by the photovoltaic effect, further, this energy drives the motor, and then the pump.
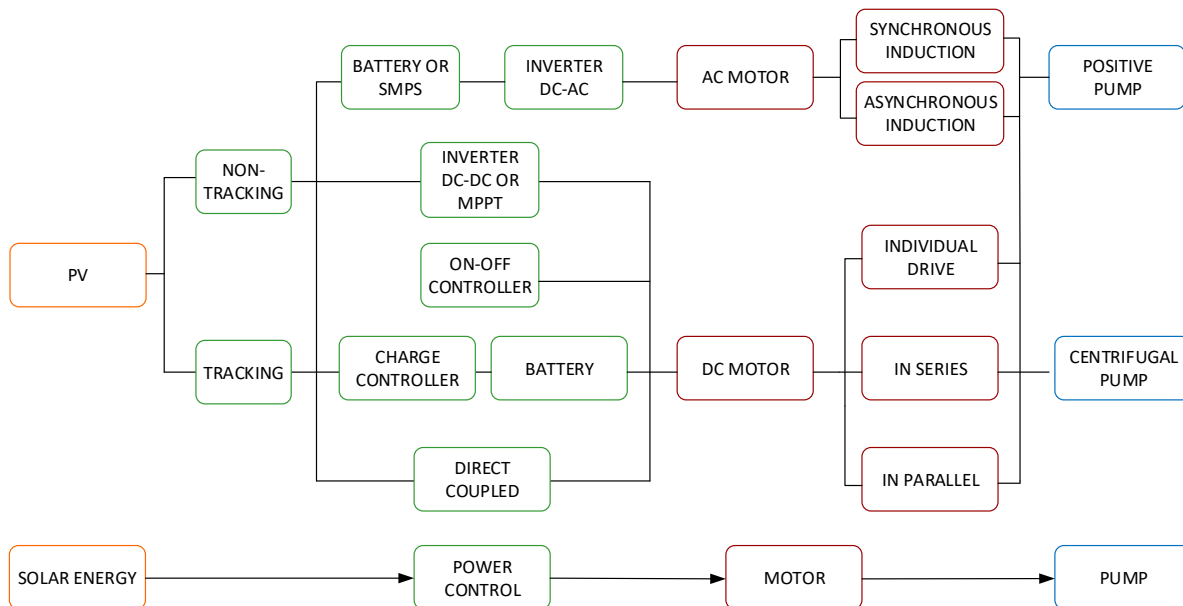
Figure 2.2: Structural outline of PVWPS, adapted from [3].

The first PVWPS were proposed in the 1970s with direct coupled DC systems [4]. However, as the solar radiation varies during the day, these systems need a MPPT algorithm and control system to proper operating.

The actual technology uses electronic systems which improve the output power and efficiency. These controllers have inputs for monitoring the pump, control the operating speed and, in some cases, also incorporate a MMPT algorithm [4]. Storage systems have been used to increase the system performance [14]. They can be designed to store electric energy in batteries, or water in a tank.

These systems are usually classified as DC or AC systems if, respectively, they are based on DC or AC motors [15], [16]. On the other hand, systems using AC motors are more attractive because of ruggedness and low cost of induction motors [16]. PVWPS are commercially available as integrated sets of components [7]. They are typically based on a PV string, a pump with a motor and a controller. Large manufactures usually provide them as closed stets of integrated components, which have an elevated cost if compared with a system based on standard and off-the-shelf components. Small or very small companies worldwide are those who install these systems.

Therefore, small companies are dependent on the dedicated system itself and on the manufacturer. Their only benefit comes from the installation and maintenance they provide to the end user. Although they cannot develop their own specific products, they can develop innovative and cost-effective prices solutions, by using off-the-shelf and widely available equipment for industry such as SFC and AC water pumps. For example, one of the cited companies in section 1.1, J.G. integrates off-the-shelf components in order to perform electric installations based on renewable energies, such as PVWPS. The other company, VALLED, develops metallic structures to support PV modules, which can be used in public lighting or for water pumping, but the system is composed by electric components from different companies.

2.2.1   PVWPS based on Standard Frequency Converters

The use of SFC in PVWPS has several advantages compared with dedicated equipment. If the pump power is of the order of magnitude of 1.5-2 kW or higher, a PV string can be directly connect to a SFC providing suitable power and voltage. There is a

great availability of SFC in the market for all power ranges. They are a reliable, off-the-shelf, and cost-effective technology, available from different manufactures, and they are practically maintenance free components [17].

A SFC consists of two power conversion stages - a rectifier bridge for AC/DC conversion and a voltage source inverter. Between them, there is a DC-link with a high DC voltage capacitor bank. In general, SFC are fed from the grid with a constant voltage and frequency, and deliver a three-phase system of variable frequency and variable voltage. Previous works have demonstrated that a PV string can be directly connected to a SFC [17],[18]. This can be implemented either using the SFC's AC input, or the DC link, as shown in Figure 2.3. In both configurations its necessary to control the DC link voltage (V_{DC}). By using the AC input, there is a voltage drop due to the diodes of the rectifier bridge, which can be avoided using the DC link configuration.
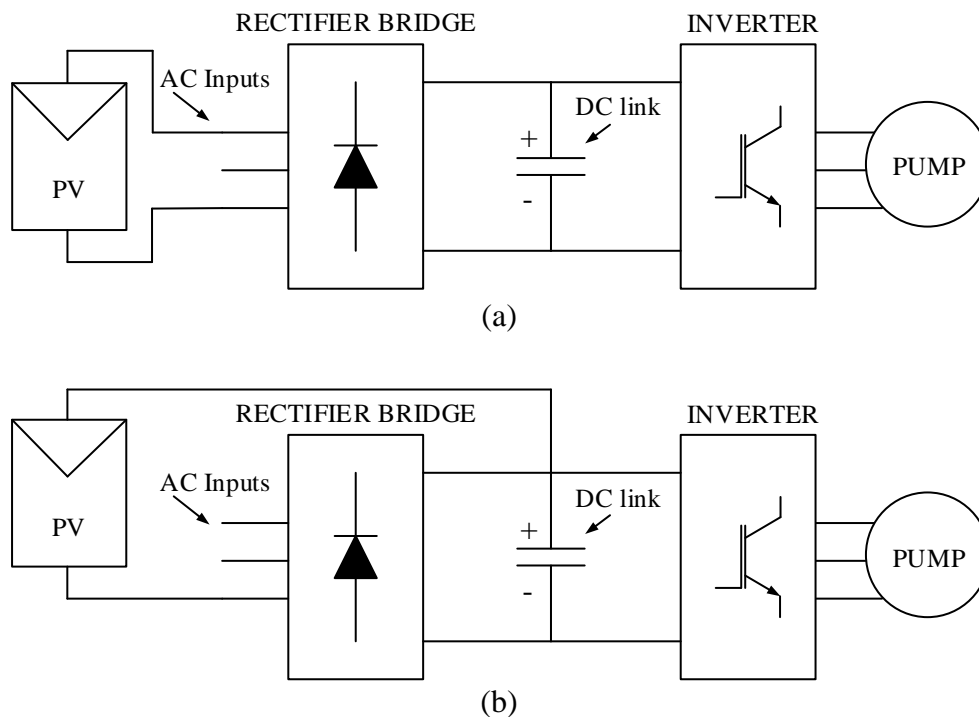
Figure 2.3: Schematic diagram of a PV directly connected to a SFC, (a) using the AC inputs, adapted from [17], (b) using the DC link input.

These devices are designed to be fed by the power grid, therefore, they need a high DC-link voltage for proper operation at rated power. If a PV string is directly connected to a SFC, the converter is supplied by a direct current and the string must supply the necessary voltage for the its operation. For example, the operation voltage ranges for single-phase and three-phase SFC ACS355, from Asea Brown Baveri (ABB), are shown in Table 2.1.

Table 2.1: ACS355 SFC rated operation voltage ranges.

	Single-phase	Three-phase
AC Input voltage	200-240 V	400-480 V
DC Link voltage	280-340 V	540-650 V

In many applications, a pump with a rated power of some hundreds of watt, operating several hours a day, is enough for water pumping requirements of several applications. Moreover, there is a natural relation between the need of water pumping systems and availability of solar radiation [3], [7], [6]. Thus, even for low power levels, PV strings need several modules to achieve the voltage levels mentioned above, as shown in Table 2.1. In practice, many installations based on AC variable speed drives have over sized PV power with additional costs in modules and supporting structure.

2.2.2 Challenges of PVWPS based on SFC

SFC have well-known adaptation challenges in PVWPS applications, such as: lack of MPPT, instability due to a sudden fall of irradiance, lack of protections against empty well and full tank states [18].

Since there is no MPPT on SFC, they must be configured to adjust the voltage/frequency proportionally to the radiance [17], [19]. Thus, the set point, i.e., the DC link operating voltage (V_{DC}) should be close to the maximum power point voltage (V_{mpp}), of the PV string, under Standard Test Conditions (STC) [17]. Considering the effect of the temperature, in applications without MPPT, the previous set point should be the voltage at the maximum temperature [18].

The DC link voltage is controlled using the so-called Proportional Integral Derivative (PID) macro included in SFC. The PID macro is used for closed-loop process control. In this case, the process variable is the DC link voltage. Thus, it is necessary to set the main control parameters, such as proportional gain (K_p), integrative time (T_i) and derivative time (T_d). In these applications, only the proportional and integrative components are needed (T_d=0) [17], [18]. The system dynamic is dependent in the radiance variation, which increases and decreases slowly during the day. Thus, the derivative component is not necessary, because there is no need to anticipate the error variation (accelerate the system's answer). It is also required to set the operating parameters, analog and digital inputs and outputs, and acceleration and deceleration times [18]. The actual value (measured DC link voltage) is given by the SFC itself, but is necessary to set it. The reference value can be set using different approaches, as described in next paragraph.

In literature, some solutions are proposed to the lack of MPPT. In [20] a simple analog MPPT tracker is used. A basic analogue circuit based on the low-cost temperature sensor LM35 is proposed in [17] to obtain the DC link voltage reference. The authors of [18] implement a MPPT algorithm and protections against a sudden fall of irradiance, empty and full tank states, however, this is done at the expense of an additional Programmable Logic Controller (PLC). A solution based on a step-up converter with MPPT algorithm, between the PV modules and SFC is proposed in [5].

Single-phase or three-phase SFC are suitable for powers of the order of magnitude of 1.5-2 kW and higher than 3-4 kW, respectively, with a single PV string. However, many applications need much lower power ranges since the amount of pumped water depends not only on the pump power but also on the number of irradiation hours. Therefore, for low power levels, in the range of some hundreds of W, the PV will be oversized in order to achieve the expected input voltage of (single-phase) SFC. For example, for a pump of 250 W, one or two PV modules could be enough, but the voltage available is too low (37-74 V) when compared with the one required to the DC link. Chapter 4 presents an approach for low power applications, using only one or two PV modules.

2.3   Water Pumps

Water pumps in PVWPS receive the mechanical energy from the motor and convert this energy into hydraulic energy of water. The mostly used pumps are submersible, centrifugal and positive displacement, as shown in Table 2.2 [3]. Their working principle is different, and each type has their own operation characteristics, that are more suitable depending on the application.

Table 2.2: Types of pumps, adapted from [3].

	Submersible	Centrifugal	Positive displacement
Characteristic	No cavitation, high discharge and head	Low head and high discharge	Used where Total Dynamic Head is high, good suction power
Drawback	Shorter life because they are inside the pond, which also difficults maintanence	Cavitation, poor suction power, priming is required	Low discharge
Working principle	Centrifugal	Centrifugal	Screw

In centrifugal pumps, suction power is produced by impeller rotation, and the casting directs the water to the outlet as the impeller rotates, as shown in Figure 2.4. This kind of pump is known as negative or non-positive displacement [3], [4]. Positive displacement pumps operate based on the Screw working principle, which is named due to it's screw shaped rotor. The working components rotate inside the chamber and trap the liquid at inlet side of the pump, then, further direct it to the outlet with high pressure [3], as shown in Figure 2.5.

For PVWPS the selection of the type of pump is dependent on the water flow requirement, height to lift the water to the tank (head) and water quality, namely clean water, hot water and sewage. For proper operation, the systems' design must meet the daily water flow and pumping head requirements [4].
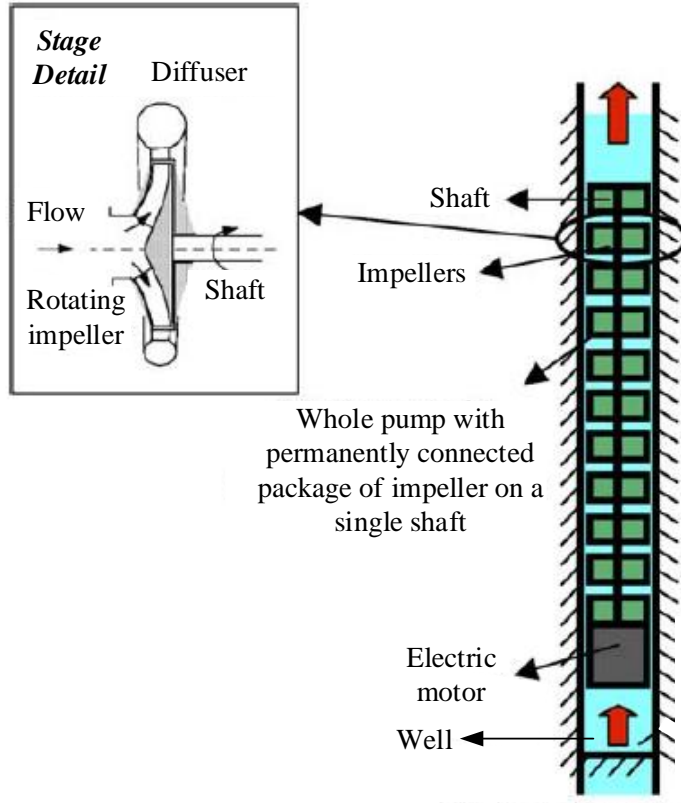
Figure 2.4: Single shaft centrifugal submersible pump, adapted from [21].
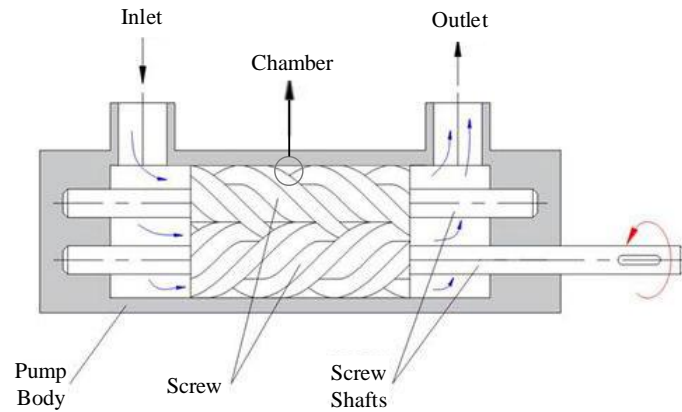
Figure 2.5: Twin screw pump, adapted from [22].

Chapter 3

Case studies of PVWPS

This chapter considers Photovoltaic Water Pumping Systems (PVWPS) applications, where the photovoltaic (PV) string is directly connected to a standard frequency inverter (SFC). Previous works have demonstrated that a PV string can be directly connected to a SFC for water pumping applications [6], [7]. Besides the advantages, described in section 2.2.1, this approach has some challenges. To further understand these approaches, three examples are presented in this chapter.

3.1 PVWPS based on SFC for 2.2-5 kW water pumps

The first example describes the challenges to design a PVWPS, which is based on direct connection of a PV string to a SFC ACS355 of 5.0 kW from ABB, to supply three-phase submersible water pumps of 2.2-5 kW.

PV modules of 250 W (REC250PE) were used, which are currently widely available in the market, and a three-phase SFC to supply the pump. To calculate the maximum number of PV modules, it is necessary to divide the SFC maximum input voltage (650 V), which is shown in Table 2.1, by the PV module Open Circuit Voltage (V_{oc}), which is 37.4 V. Thus, the maximum number of PV modules is 17 (650V/37.4V = 17.38). This number of modules supplies the SFC with a voltage of 635.8 V (17x37.4 V = 635.8 V). However, this results in an over sized PV power, because the power required by the load

is of 2.2 kW, and the calculated PV power is 4250 W (17x250 W = 4250 W).

If the PV power is estimated to be equal the load power, - considering a hypothetic situation which it would supply the SFC with the required voltage level - the pump would run only during the peak generation period. However, in this example, the load power (2200 W) represents only 51.76% of the installed PV power (4250 W), as shown in Figure 3.1. Thus, the system is suitable over sized because the pump would run from 8:45 a.m. until 16:05 p.m., approximately seven hours, assuming for instance, a real data of radiance levels, of Bragança - Portugal, (Figure 3.1).
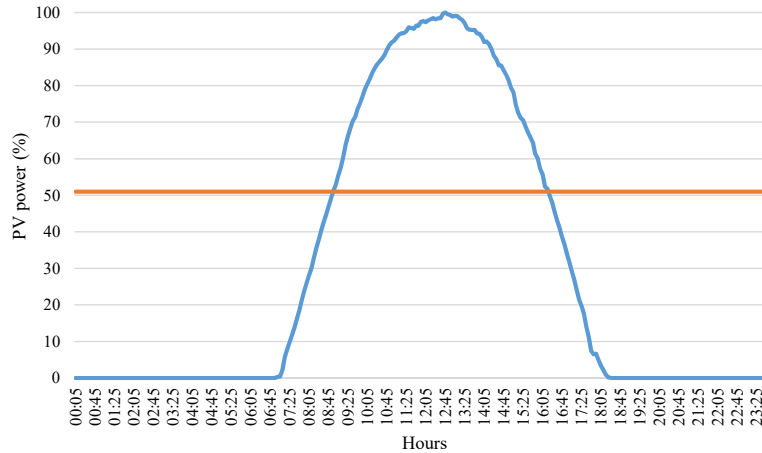
Figure 3.1: PV power vs hours. Adapted from [23].

For a load power higher than 2.2 kW, this strategy is interesting, but for lower power levels the PV power oversizing increases considerably. This is described in the next two sections with examples of the challenges to design systems for lower power pumps.

3.2   PVWPS based on SFC for 1-2 kW water pumps

This example also considers a PVWPS directly connected to a SFC, using a three-phase submersible water pump with a power range between 1-2 kW.

To supply the SFC, the same PV modules of the previous example were chosen, with nominal power of 250 W, and V_{oc} of 37.4 V. The pump is driven by a three-phase SFC ACS355 of 1.5 kW from ABB. Although, the SFC power is half of the previous example,

the required input voltage is the same. Thus, the maximum number of PV modules was calculated, which is also 17 (650V/37.4V = 17.38). To reduce the number of PV modules, a single-phase (input) SFC ACC355 from ABB can be used. The required voltage level of this SFC, which is lower than the three-phase model, is shown in Table 2.1. Considering this, the calculated maximum number of PV modules is 9 (340/37.4 = 9.09). These PV modules supply the SFC with a voltage of 336.6 V (9x37.4 V = 336.6 V). The total PV power is 2250 W (9x250 W = 2250 W). This is still an over sized PV power, considering the load (1.5 kW), however, it is inferior than the case using a three-phase SFC. This strategy was tested in laboratory. A single-phase input SFC, has an output voltage that depends on the input voltage. In this case it is not possible to run the pump at the nominal speed, because it is supplied with a under-voltage level.

This strategy can be suitable with/for a pump running with a limited speed, which is lower than the nominal value, but still suppling the required water flow. An alternative can be a single-phase input and output SFC, as described in the next section.

3.3 PVWPS based on SFC up to 1.0 kW water pumps

This example is designed for a single-phase submersible pump of 1.1 kW from Ideal Delta, which is available at the laboratory. The pump was driven by a Variable Speed Drive (VSD) of 1.5 kW. The VSD has a single-phase input and a single-phase output, but these SFC are not so widely available in the market. To achieve the required VSD's input voltage, the same PV modules (REC250PE) of the previous examples were used. The calculated number of maximum PV modules is 9 (340V/37.4V = 9.09). These PV modules supply the SFC with a voltage of 336.6 V (9x37.4 V = 336.6 V) and the total PV power is 2250 W (9x250 W = 2250 W). This strategy requires the same PV power of the example for a 1.5 kW pump, i.e., even with the reduction of load power, the required voltage at the input of the VSD results in a considerable over sized PV power.

For many applications where a small pump is required, e.g., 350 W up to some hundreds of W, directly connected PVWPS are considerably over sized, due to the required

SFC input voltage. Thus, it is necessary to provide a set of components to rise the PV output voltage, reducing the required number of PV modules to supply this voltage level.

As means of comparison, if two PV modules of 250 W were direct connected to a SFC, with V_{oc} of 37.4 V, it would supply 75 V (2x37.4 V = 74.8 V). This voltage is lower than the SFC required for proper operation. Thus, a new approach for low power PVWPS applications is proposed in the next chapter.

Chapter 4

A New Approach Proposal for Low Power PVWPS

A new approach for low power applications based on standard components is presented in this chapter. A suitable speed control technique was developed to follow the solar radiation.

4.1   Description of the Proposed System

For applications of low power PVWPS (some hundreds of Watts), where one or two PV modules have enough installed capacity, an innovative solution can be developed, still based on SFC and other conventional equipment. The proposed approach is shown in Figure 4.1, where only one PV module of 250 W (Rec 250PE) is used due to a set of components used to raise the PV output voltage, which will be explained in the following paragraphs.

Projects of PVWPS are designed to meet the load, or the water requirement, depending on the application, such as crop irrigation, small communities or families supply. Thus, the components used for the approach will be described starting with the pump and the SFC.

The vast majority of SFC has a three-phase output, they are designed to supply a

three-phase load. However, for low power applications, submersible pumps are usually single-phase. It is possible to supply this kind of pump with a three-phase supply, but there are several drawbacks, such as overheating and phase imbalance (one phase has double current, compared with the two others). Another alternative is to use a starting or permanent capacitor, but it is necessary an external connection or a system to switch off the permanent capacitor. Both situations were verified in laboratory tests with a standard water pump and SFC. It was used a single-phase submersible water pump (1.1 kW) from Ideal Delta, driven by a single-phase input SFC from ABB, model ACS355-01E-07A5-2 (1.5 kW).

There are VSD for single-phase load, but they are not widely available in the market, although it is a mature technology. Therefore, a SFC for three-phase load was selected. To reduce the required input voltage, shown in Table 2.1, it was used a single-phase input SFC for low power applications (370 W).

In order to evaluate low power water pumps, driven by a three-phase SFC, a three-phase surface centrifugal pump (350 W) was selected to validate the proposed approach.

The PV's output voltage (37 V), can not supply SFC's required input voltage, that is between 280-320 V. Thus is necessary to use a component, or a set of components to rise the voltage level. One equipment widely available nowadays is a DC/AC battery inverter for stand alone applications. These components are widely available and low cost. Some models have square wave output, which reduce their price and can be directly connected to SFC's rectifier bridge. However, is necessary a low cost solar battery charger, with MPPT, and a battery. Indeed, the battery is used, because it was verified in laboratory test that the charger require a battery and also the battery inverter. Although this strategy requires a battery, its storage capacity can be reduced. This is achieved designing the system to storage water in a tank, rather than energy in the battery. The charge controller are off-the-shelf and low-cost components, they are need to charge the battery with its required voltage level. This voltage level is different depending on the Depth of Discharge (DOD). In this proposed approach, the battery is used only as a voltage buffer. This will be described in subsection 4.1.1.

An alternative to the battery inverters described above, can be developed using a low power DC-AC power modules for PV stand alone applications, which are available on the market at low cost (less than 15 Euros). An example is the push-pull DC-AC inverter, shown in Figure 4.2, with a pulse transformer to rise the voltage. The output voltage consists of pulses generated by a Pulse Width Modulation (PWM) signal, with a switching frequency of 20 kHz. Even though the SFC has a rectifier bridge at the input, it is not capable of rectifying the high frequency pulses provided by the push-pull inverter. Thus, a rectifier bridge with Schottky, that are high frequency diodes, is applied between the DC-AC inverter and the SFC, as shown in Figure 4.2. By using this circuit, a DC output voltage of 312 V is generated from the range of 12-14 V input voltage. The maximum output power is 500 W.
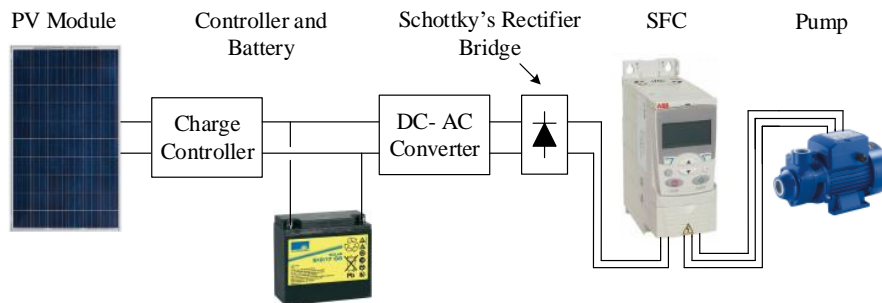

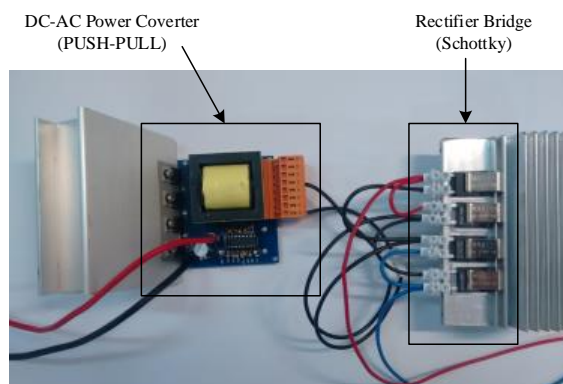Figure 4.1: Illustration of the proposed solution.

Figure 4.2: Push-pull DC-AC inverter and rectifier bridge based on fast diodes.

Without this set of components, in a direct connection of the PV module with the inverter, the supplied voltage would be the PV's open circuit voltage (V_{oc}) (37,5 V), which is much inferior than the SFC's minimum input voltage, as shown in Table 2.1. Therefore, in order to achieve the SFC's minimum input voltage, would be necessary an over sized PV power, as described in chapter 3.

4.1.1   Battery Voltage Control

The battery can be sized with two different objectives. On the one hand, a high capacity is necessary if the option is to store electric energy instead of storing water in a tank. On the other hand, a very low capacity can be used if the option is to store water instead of electricity. This work is focused on the latest option. Therefore, the cost of the battery is reduced. This approach uses a suitable control strategy through the PID macro of the SFC that strongly increase the battery lifetime. Indeed, the battery is used only to enable the operation of the system and not to store energy.

Even in a small battery, it is possible to increase the number of life cycles and, thus, its lifetime. This is done by limiting the DOD of the battery to 20%. With this percentage, is possible to achieve approximately the maximum number of cycles, approximately 3800 cycles as shown in Figure 4.3. Limiting the DOD to a higher level, for example 40%, the number of life cycles decreases considerably, approximately 1600.
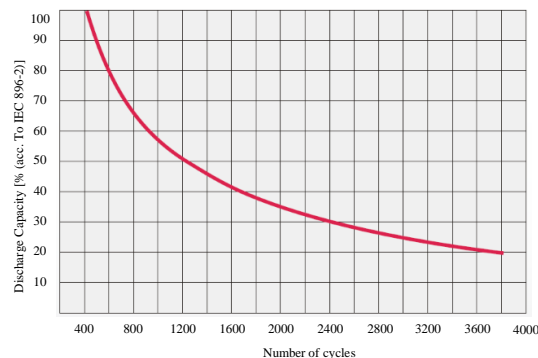

Figure 4.3: Number of Cycles vs. Depth of Discharge (DOD). Adapted from [24].

This strategy can be implemented using the SFC PID macro for a closed loop control of the pump's speed, and setting a high battery voltage as reference value, as shown in Figure 4.4.
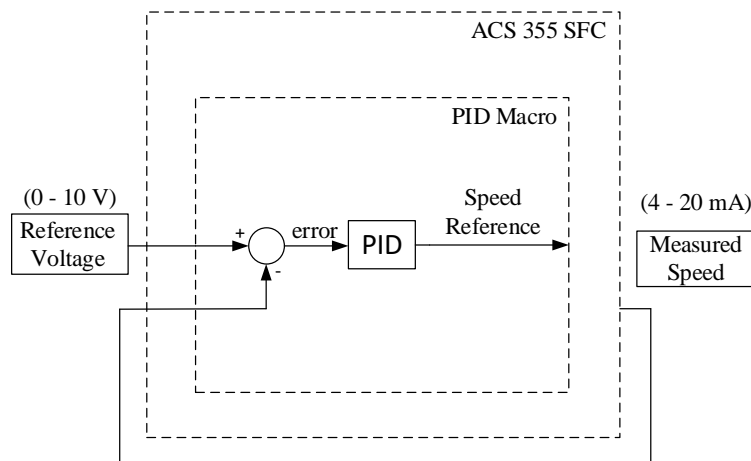
Figure 4.4: Battery voltage (speed) control.

The SFC itself gives the actual value (speed of the pump). This is used as input of the PID control, which is compared with the reference voltage (the battery voltage), which is explained in section 5.1.1. These signals (inputs), are suitable scaled in order to be compared. Thus, the SFC is parametrized in order that the battery voltage is a reference for speed of the pump, this is further explained in section 5.1.2. Therefore, the pump's speed follows the battery voltage, increasing or reducing the values, as a result of the radiation variation.

Thus, the main parameters to be set, in the PID macro, are the proportional gain and the integral time, K_p and T_i respectively. The derivative time (T_d) is zero, because there is no need to anticipate the error variation of the system, as explained in section 2.2.2. According to test implemented on the experimental platform, described further, in chapter 5, the SFC PID parameters were set by trial and error, as shown in Table 4.1.

Table 4.1: Main PID Parameters

SFC Parameter Group 40 - PID		
Number	Name	Value
4001	PID Gain	Kp = 1
4002	Integrative Time	Ti = 2 s
4003	Derivative Time	Td = 0 s
4023	PID Sleep Level	19 Hz
4024	PID Sleep Delay	10 s
4026	PID Wake-Up Delay	60 s

Based on the configured parameters, the system is shut down when the V_{bat} is less than 80%. This is obtained setting the PID Sleep Level parameter to 19 Hz, which corresponds to the battery's minimum operation voltage, as shown in Figure 4.5. Therefore the pump's speed dynamics vary between the defined minimum value (19 Hz) and maximum value, in other words, between approximately 1000-2800 rpm. The main operation and configuration characteristics of the proposed system are presented in this chapter.
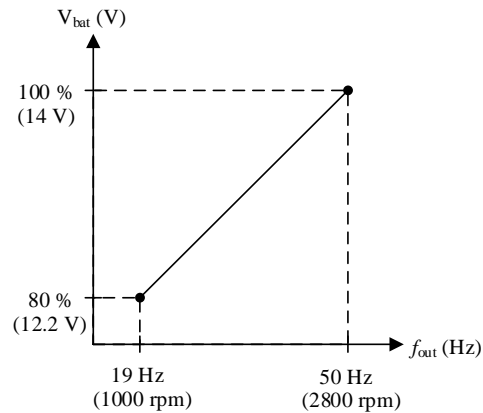
Figure 4.5: V_{bat} vs f_{out} relation.

Chapter 5

New Approach Validation

This chapter presents the experimental platform and describes the used components. Then, the experimental results are presented and discussed.

5.1 Experimental Platform

The validation of the proposed approach for low power PVWPS was achieved using an experimental platform based on the components described in Table 5.1 and shown in Figure 5.1.

The speed of the pump is controlled through the standard frequency converter (SFC) by the battery voltage, which is given by the battery charger according to the irradiation. The maximum speed is obtained for the maximum battery voltage and the minimum speed was set to 80% of this value. This performance is obtained by a suitable parametrization of the PID macro and analogue inputs and outputs of the SFC. This battery utilization strategy decrease the Depth of Discharge (DOD) and, therefore, increases the number of life cycles and, hence, improve its lifetime. Furthermore, the battery has also advantages. Namely, the presence of the battery mitigates the instability due to a sudden fall of irradiance. In fact, the SFC does not feel directly a sudden lack of irradiance anymore.

Table 5.1: Equipment used in the experimental platform.

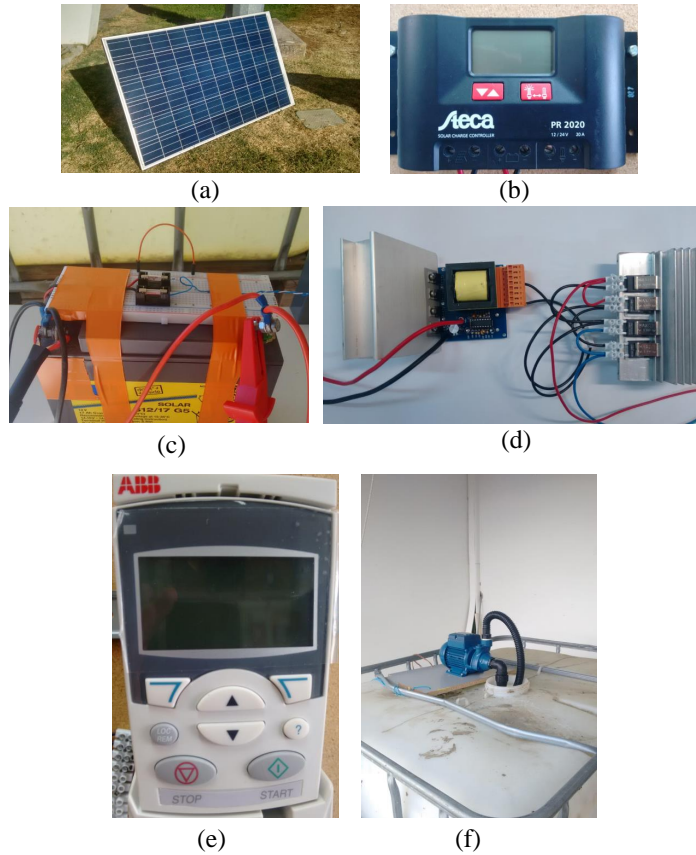| Component	Equipment Used
Photovoltaic Module	REC 250PE Q2
Charge Controller	Steca PR2020
Battery	Ultracell UCG 20-12
DC-DC Power Converter	Push Pull Converter
Rectifier Bridge	Schottky DSEI 30-10 AR
Standard Frequency Converter	ABB ACS355-01E-02A4-2
Surface Pump	Pentax PHT45 350 W

Figure 5.1: Experimental platform components, (a) PV module, (b) charge controller, (c) battery and components to scale its voltage, (d) DC-DC power converter and rectifier bridge, (e) single-phase SFC ACS355, (f) water pump and tank.

5.1.1 Battery Voltage Acquisition

As described in section 4.1.1, the pump's speed (ω_{pump}) will be controlled according to the battery voltage (V_{bat}) level. This is done using the PID control macro of the SFC. In the following paragraphs, it is described how this strategy was implemented. At full charge, V_{bat} is approximately 14.4 V, and at 80% of its storage capacity, or state of charge (SOC), it is approximately 12.2-12.3 V, it was verified during laboratory tests. Most of the SFC has analog inputs/output for control purposes. However, the SFC analog input voltage range is 0 - 10 V, e.g., analog input AI 1. Thus, a voltage divider was used to set V_{bat} to the appropriate voltage range, i.e., the reference voltage (V_{Ref}), as shown in Figure 5.2.
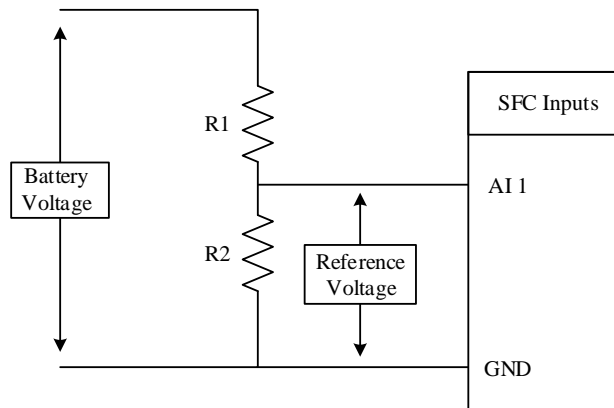

Figure 5.2: Battery voltage measurement.

The required output voltage, or in this case, the V_{Ref} was calculated using Equation 5.1.

$$V_{Ref} = \frac{V_{bat}R_2}{R_1 + R_2} \tag{5.1}$$

Using the required value of V_{Ref}, which is 10 V, and V_{bat}, 14 V, in Equation 5.1, the result is:

$$10 = \frac{14R_2}{R_1 + R_2}$$

Isolating R_1 is the last equation, the result is:

$$R_1 = \frac{4R_2}{10} \tag{5.2}$$

Based on the relation shown in Equation 5.2, is possible to calculate the required resistance values. R_2 was set using a potentiometer of 10 kΩ, applying this to Equations 5.2, the result is:

$$R_1 = \frac{4 \times 10k}{10} = 4k\Omega$$

However, these are the resistance theoretical values. The used resistance values were $R_2 = 9.7$ kΩ, and $R_1 = 4.7$ kΩ. This was done, due to the restriction of the commercial values, available, for the resistors. Applying this resistance values in Equation 5.1, the result is:

$$V_{Ref} = \frac{14 \times 9.7k}{4.7k + 9.7k} \approx 9.43V \tag{5.3}$$

Thus, considering Equation 5.3, the relation between V_{bat} and V_{Ref} is described in Equation 5.4. This relation according to the battery SOC, is shown in Table 5.2.

$$k = \frac{14}{9.43} \approx 0.67 \tag{5.4}$$

Table 5.2: V_{bat} and V_{Ref} relation.

SOC	V_{bat} (V)	V_{Ref} (V)
100%	14.0	9.430
80%	12.2	9.174

In Figure 5.2, V_{Ref} is applied between SFC's analog input, AI1 and GND. This voltage value, is used as the reference for the PID macro to control ω_p (subsection 4.1.1).

5.1.2 SFC Parameters

The parameters that were set in the PID macro to control the battery voltage, were explained in section 4.1.1, and shown in Table 4.1. However, these are not the only parameters that were set specifically for this application. The remaining groups of parameters and the reason why they were used, is described in this section.

The remaining PID parameters are set in group 40, as shown in Table 5.3. These parameters define what pins were used for the reference and actual value of the control process, how is activate the PID Sleep and which of the PID groups was used.

Table 5.3: Remaining PID Parameters.

SFC Parameter Group 40 - PID		
Number	Name	Value
4010	Setpoint	AI 1 (1)
4014	Feedback	ACT 1 (1)
4016	ACT 1 Input	AI 2 (2)
4022	Sleep	Internal (7)
4027	Parameter PID	PID SET 1 (0)

Furthermore, it is necessary to set the group 11 (Reference select), as shown in Table 5.4. This group defines the inputs of the PID's variables (reference and actual value).

Table 5.4: Reference Select Parameters.

Reference Select Group 11		
Number	Name	Value
1101	Keypad reference	Ref 2(%) (2)
1102	External ref	EXT 2 (7)
1103	Ref 1 Select	AI 1 (1)
1106	Ref 2 Select	PID 1 OUT (19)

After the PID and reference parameters, the first group of parameters that has to be set is the Start-Up Data. These parameters define the language, the macro which will be used, the control mode and the motor characteristics, as shown in Table 5.5.

Table 5.5: Start-Up Parameters.

Start-Up Data Group 99		
Number	Name	Value
9901	Language	Portuguese (5)
9902	Macro	PID Control (6)
9903	Motor Type	Am (1)
9904	Ctrl Mode	Scalar (3)
9905	Motor Voltage	230 V - Δ connected
9906	Motor Current	1.73 A
9907	Motor Freguency	50 Hz
9908	Motor Speed	2800 rpm
9909	Motor Power	370 W

The SFC analog inputs and outputs, groups 13 and 15 respectively, were set according to the SFC's Input/Output connections, as shown in Figure 5.3. V_{Ref} is applied between analog input 1 (pin 2 - AI 1) and GND (pin 3). In this case V_{Ref} is the reference value of the PID control process, as described in section 5.1.1. AI 1 is set in parameter's group 13 (analog inputs, Table 5.6).

The actual value of the PID control process is applied in the analog input 2 (pin 5 - AI 2) by the analog output (pin 7 - AO). The AO signal, between 0-20 mA, which corresponds to the motor (pump) speed, is set in parameter group 15 (analog output, Table 5.7).

1	SCR	Signal cable shield (screen)
2	AI 1	Process Reference Voltage: 0...10 V
3	GND	Analog circuit common
4	+10V	Reference voltage: +10 VDC, max 10 mA
5	AI 2	Process actual values: 4...20 mA (PID)
6	GND	Analog circuit common
7	AO	Motor Speed values: 0...20 mA

V_{ref} is applied between pins 2 and 3.

Figure 5.3: Input/Output Connections. Adapted from [25].

In group 13 (analog inputs), it is set the operation value that corresponds to AI 1 and AI 2 input signals, which are 0 - 10 V and 0 - 20 mA respectively. For AI 1, the minimum

value is set to 80%, the maximum value is set to 87%, in order to match the operating range of V_{Ref}, which was described in section 5.1.1. AI 1 signal range from 80% to 87%, corresponds to 8.17 V and 8.7 V respectively, as shown in Table 5.2.

Table 5.6: Analog Inputs Parameters.

Analog Inputs Group 13		
Number	Name	Value
1301	Minimum AI 1	80 %
1302	Maximum AI 1	87 %
1304	Minimum AI 2	0 %
1305	Maximum AI 2	100 %

This means that the maximum values of V_{Ref} represents 87% of AI 1 signal. The minimum value of V_{Ref}, which represents 80% of the battery state of charge, is represented by 80% of AI 1 signal, as shown in Figure 5.4. The pump speed control based on the battery voltage level was described in section 4.1.1
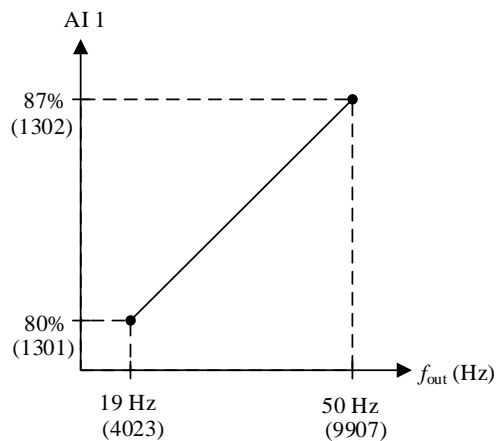
Figure 5.4: V_{Ref} vs f_{out}.

In group 15 (analog output), shown in Table 5.7, it is set what represents AO1 (output signal). In this case the AO was set to give the motor (pump) speed.

Table 5.7: Analog Outputs Parameters.

Analog Outputs Group 15		
Number	Name	Value
1501	AO1 Content Select	Speed (102)
1502	AO1 Content Min	0 rpm
1503	AO1 Content Max	2800 rpm
1504	Minimum AO 1	0 A
1505	Maximum AO 1	20 mA

5.2 Experimental Results

Tests were performed, aiming to validate the system operation under different real conditions.

5.2.1 Test A - System under continuous operation (push-pull)

This test aims to verify the pump's speed variation based on the battery voltage level.

The test was carried out with one PV module, REC250PE of 250 W, on the outside of the laboratory. The module orientation (35°, south) and angle (16°), were the same of a PV string installed on the roof of the laboratory. The test was performed on October 23th, 2018, under variable solar irradiation and temperature levels, acquired by the measuring systems present in the laboratory. The system scheme is shown in Figure 5.5. The measured variables were: I$_{pv}$; the battery voltage (V_{bat}), the V$_{Ref}$, the V$_{DC}$, the ω_p and I$_p$. The values of I_{pv}, V_{bat}, V_{DC} and V_{Ref} were measured with the multimeter 734-01 from YOKOGAWA. The value of ω_p and I_p were given by the SFC itself. The complete data is shown in Table A.1, which is in appendix A.

To verify the ω_p variation according to the irradiance, the data of the radiance level, from Table A.1, was used to plot the Figure 5.6. The irradiance curve increases during the morning and reaches its peak at approximately at 12:40 hrs. It decreases during the afternoon and is zero after 18:00 hrs. At 13:20 hrs, it is verified a variation from 900 W/m² to 600 W/m², due to a cloud passing in front of the PV module.

Using the data of ω_p and V_{bat} from Table A.1, the Figure 5.7 was plotted. The
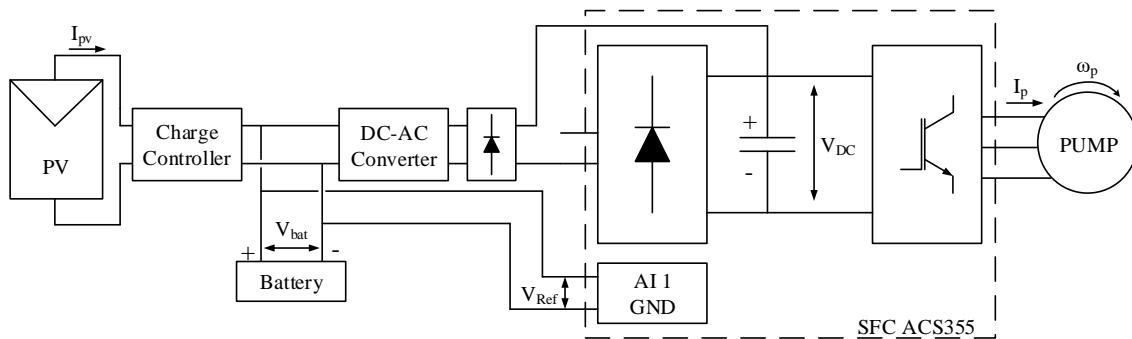
Figure 5.5: System scheme - Test A.

pump's speed curve show expected results for the operation of the system, with ω_p varying according to the battery voltage. That occurs, due to the PID control described in section 4.1.1. Moreover, due to the battery that was used, system is robust to small irradiance variations, such as at 13:20, shown in Figure 5.6, and that ω_p is stable during this period, as shown in Figure 5.7.
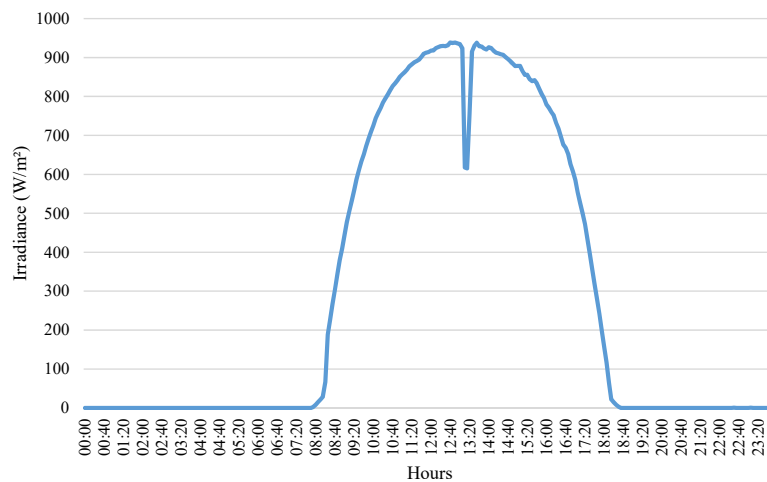

Figure 5.6: Irradiance levels over the day.

Furthermore, is possible to verify that the system works continuously while the power generated by the PV module is sufficient to keep the battery charged above 80%. In Figure 5.7, is verified that this occurs until 16:15 hrs. After this moment, the system works intermittent, because it shuts off when the battery voltage reaches 80% of its value,
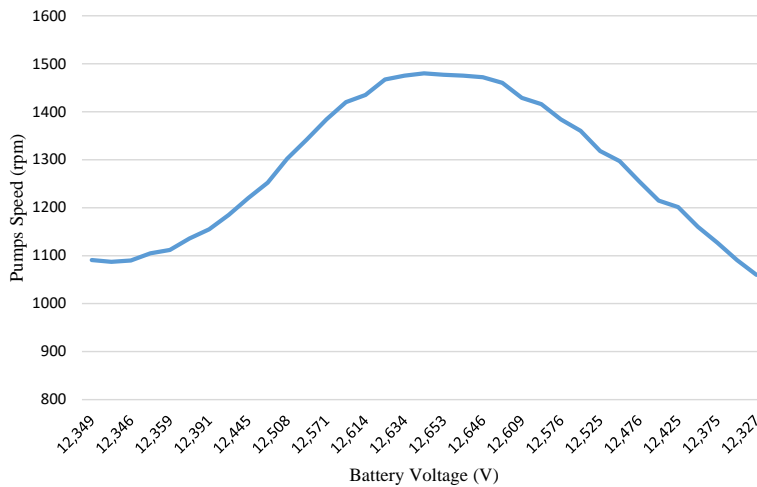
Figure 5.7: Pump speed vs. battery voltage.

and tries to automatically re-start every 60 seconds. If, in this time interval, the power generated by the PV module is sufficient to charge the battery above 80%, the systems re-starts, otherwise, after 5 attempts it will turn off permanently. The system remains off until the power generated by the PV module charges the battery above 80%. This strategy was implemented using the SFC's inputs/outputs and the PID macro. The system shut down limit of 80% was based on V_{Ref} voltage level, as explained in subsection 5.1.1, and was represented in Figure 5.4. The re-start time was set in parameter 4026, as described in subsection 4.1.1 and shown in Table 4.1.

The maximum value presented by the speed in Figure 5.7 is 1480 rpm, which is less than the nominal speed of the pump (2800 rpm). This happens because in the DC-AC (push-pull) power module, there is no control system of the output voltage. In load conditions, this voltage (215-220 V) is inferior than the recommended to supply the SFC, that is 280 V. Since the input voltage of the inverter V_{DC}, is lower than the recommended level, thus, the pump is supplied with sub-voltage and does not operate with the rated speed.

5.2.2   Test B - System with battery inverter AJ

This test aims to verify the system operation using a battery inverter instead of the push-pull module. The test was carried out using the same components of the previous one, except the push pull module that was replace by a battery inverter from Studer, model AJ275-12 sine wave, shown in Figure 5.8.

Figure 5.8: Battery Inverter.

The module orientation (35°, south) and angle (16°), were the same. The test was performed on October 25th, 2018, under variable solar irradiation and temperature levels, acquired by the measuring systems present in the laboratory. The system scheme is shown in Figure 5.9, the difference from Test A is that in this test the battery inverter is connected to the SFC's rectifier bridge, due to the its synchronous wave form.
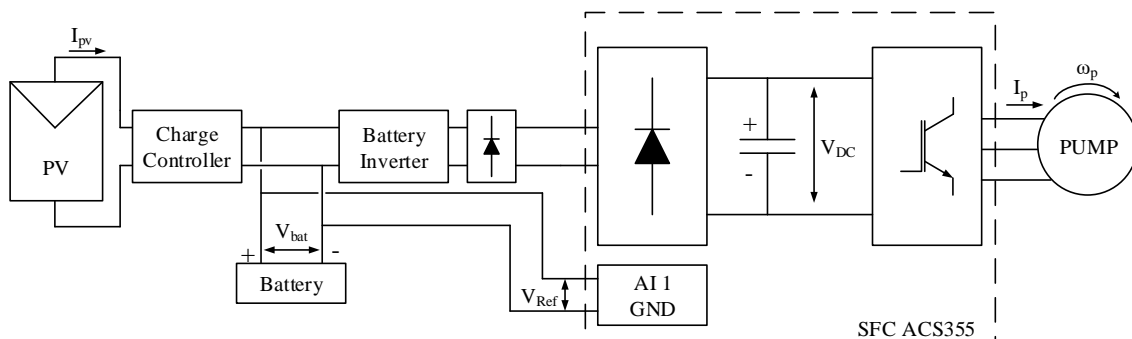

Figure 5.9: System scheme - Test B.

The measured variables were the same of the previous test, which were described in section 5.2.1. The complete data of this test is shown in Table A.2, that is in appendix A.

To verify the variation according to the irradiance, the data of the radiance level, from Table A.2, was used to plot the Figure 5.10. The irradiance increases during the morning and reaches its peak approximately at 12:40 hrs. It decreases non-linearly during the afternoon and is zero after 18:00 hrs. The irradiance oscillations occurs due to changes in weather conditions and also passing clouds.

Figure 5.10: Irradiance levels over the day.

Using the data of ω_p and V_{bat} from Table A.2, the Figure 5.11 was plotted. The pump's speed curve does not show expected results for the operation of the system, and not vary according to the irradiance levels during the day. In the start, ω_p decreases linearly following the battery discharge, as seen in the horizontal axis. After this, the battery charges and discharges repeatedly, because, the current that the battery inverter requires from the battery is higher than the current received by the battery from the charge controller. The oscillations are not periodic due to the irradiance variations, as shown in Figure 5.10. The reason for these oscillations, in battery charge and discharge, are further discussed in subsection 5.2.4.
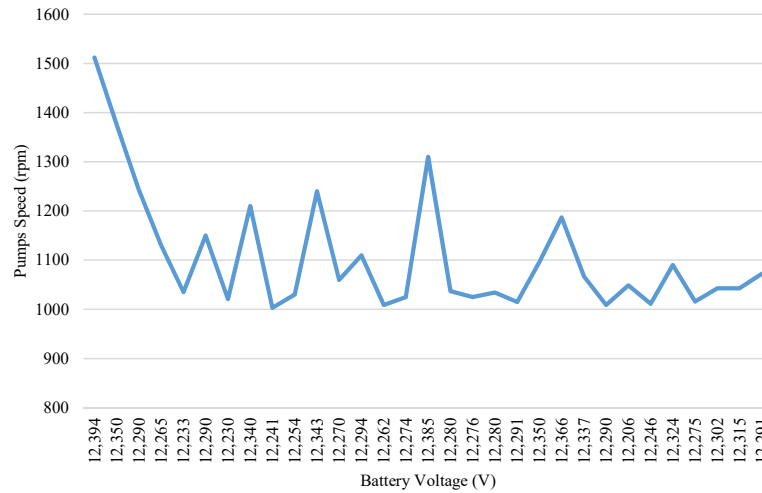
Figure 5.11: Pump speed vs. battery voltage.

5.2.3   Test C - Battery inverter AJ using 2 PV modules

This test aims to verify the system operation with the battery inverter using two PV modules. The test was carried out with two PV modules, REC275PE of 275 W, connected in parallel on the outside of the laboratory. The module orientation (35°, south) and angle (16°), were the same of the previous tests. The test was performed on November 3rd, 2018, under variable solar irradiation and temperature levels, acquired by the measuring systems present in the laboratory. The system scheme was the same of the Test B, shown in Figure 5.9. The measured variables were the same of the previous tests, which were described in section 5.2.1. The complete data of this test is shown in Table A.3, that is in appendix A.

To verify the variation according to the irradiance, the data of the irradiance level, from Table A.3, was used to plot the Figure 5.12. The irradiance increases during the morning and reaches its peak approximately at 11:20 hrs, after this, there is a sudden fall of irradiance to approximately 100 (W/m²), due to a passing cloud. At 12:40 hrs, it decreases non-linearly until 15:20 hrs, and after that decreases linearly and is zero after 18:00 hrs. These oscillations occurs due to changes in weather conditions and also passing clouds.
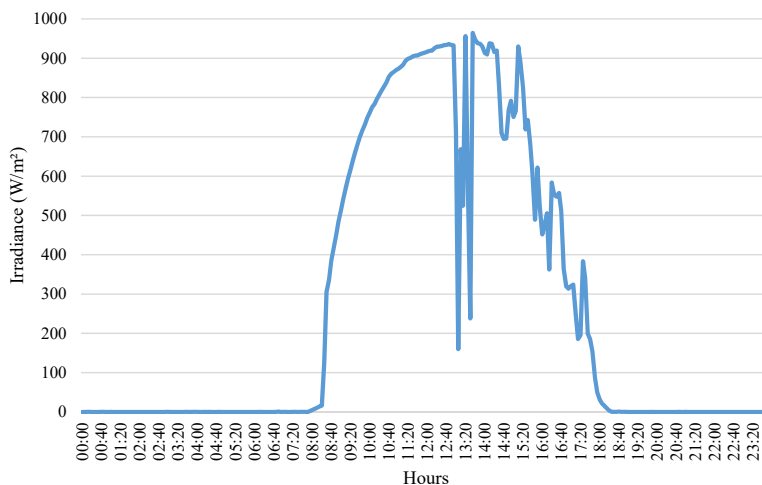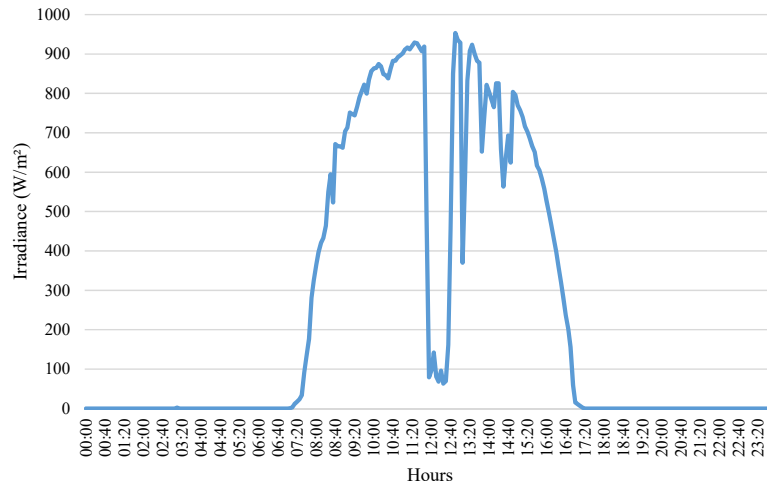
Figure 5.12: Irradiance levels over the day.

Using the data of ω_p and V_{bat} from Table A.3, the Figure 5.13 was plotted. The pump's speed curve show expected results for the operation of the system, with ω_p varying according to the battery voltage. That occurs, due to the PID control described in section 4.1.1. Moreover, due to the fact that two PV modules were used in parallel, I_{pv} is double the values of the test A and B, its reduce the difference in the current fed by the charge controller to the battery, and the current required by the battery inverter from the battery. This results in a more stable system, as seen in ω_p operation.
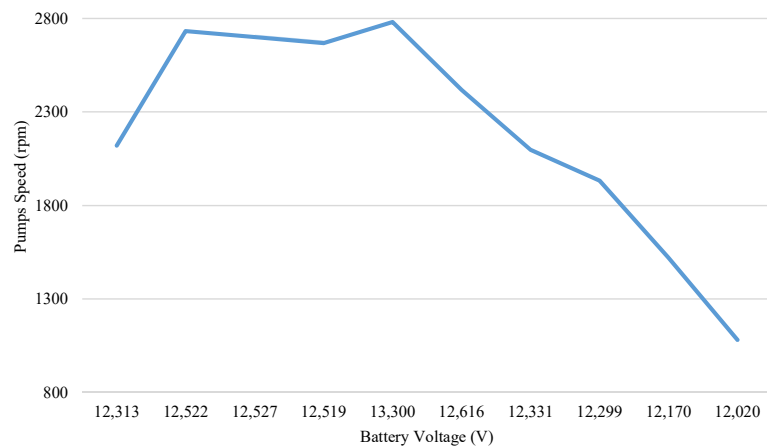
Figure 5.13: Pump speed vs. battery voltage.

5.2.4 Test D - Comparison of required current from three inverter components

This section, aims to discuss and compare the required current from the push-pull (Figure 4.2), the battery inverter AJ275-12 (Figure 5.8) and inverter COTEK 600 (Figure 5.14) to supply the pump.

Figure 5.14: Inverter Cotek 600 W.

The test was carried out with one PV module, REC250PE of 250 W, outside of the laboratory. The module orientation (35°, south) and angle (16°), were the same of the previous tests. The test was performed on November 13th, 2018, under variable solar irradiation and temperature levels, acquired by the measuring systems present in the laboratory. The system scheme is shown in Figure 5.15. In this figure the 'Inverter Component' represents the different components that were used and compared in this test.

Figure 5.15: System scheme - Test D.

The measured variables were the same of the previous tests, except temperature. The battery input (I_{bat-in}) and output currents ($I_{bat-out}$) were acquired. The complete data of this test is shown in Table A.4, that 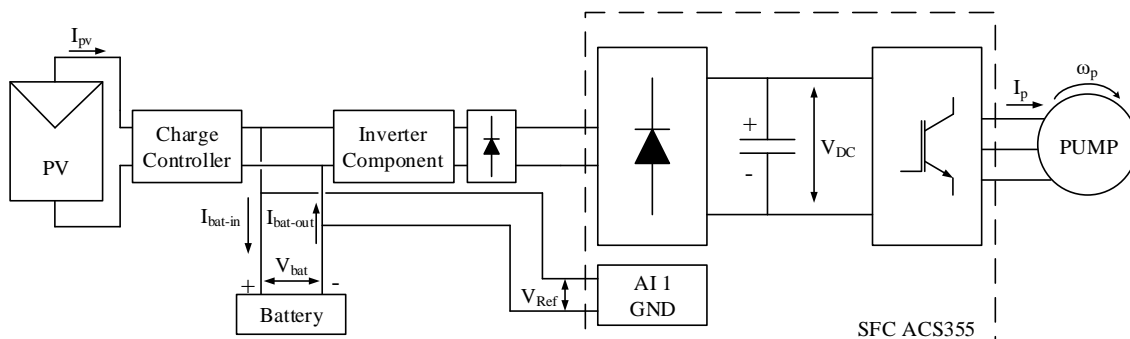is in appendix A. The value of I_{bat-in} was measured by the charge controller, $I_{bat-out}$ was measured with the power quality analyzer FLUKE 43, due to its high current range, that are above 20 A.

The data of irradiance level, from Table A.4, was used to plot the Figure 5.16. The irradiance curve oscillates during the day due to changes in weather conditions and passing clouds. The test was realized in the afternoon, because after 13:30 hrs the irradiance was more stable.
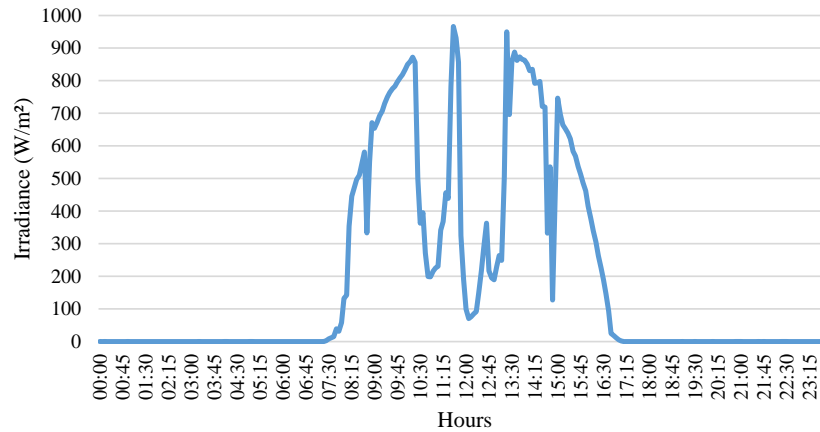
Figure 5.16: Irradiance levels over the day.

Battery inverter AJ

Using the data of V_{bat} and ω_p from Table A.4 (battery inverter AJ 240 VA), the Figure 5.17 was plot. The V_{bat} does dot vary according to the solar irradiance level, and is not the related to the actual state of charge of the battery, this is due to two factors: a) the I_{bat-in} value is inferior than $I_{bat-out}$, thus, in this situation the battery is constantly discharging; b) the charge controller's MPPT algorithm can impose a high voltage in the battery (V_{bat}), in order to charge it, such it seems to happen in 13:15, 13:30 and 13:40, but is not able because $I_{bat-out}$ is almost two times higher than I_{bat-in}. This means the peak points of V_{bat} does not represents an increase in the solar irradiance level.

The ω_p curve shows expect results, varying according to the V_{bat}.
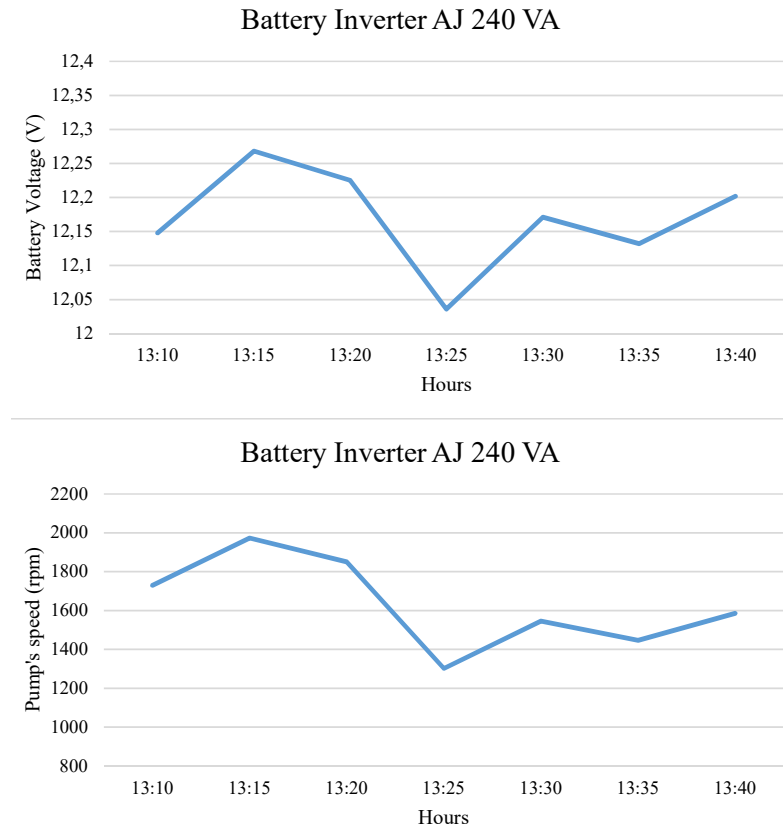
Figure 5.17: V_{bat} and ω_p levels over the afternoon.

Push-pull converter

Using the data of V_{bat} and ω_p from Table A.4 (Push-pull converter), the Figure 5.18 was plot. The V_{bat} shows expected results. It decreases linearly because I_{bat-in} is inferior than $I_{bat-out}$, but, the difference between the values is smaller if compared with results obtained in the test using the battery inverter AJ, as shown in Table A.4. The push-pull requires less current from the battery, i.e., the losses are inferior. This is due to constructive aspects, the push-pull uses a pulse transformer and the battery inverter AJ uses a standard transformer. The ω_p curve shows expect results, varying according to the V_{bat}.
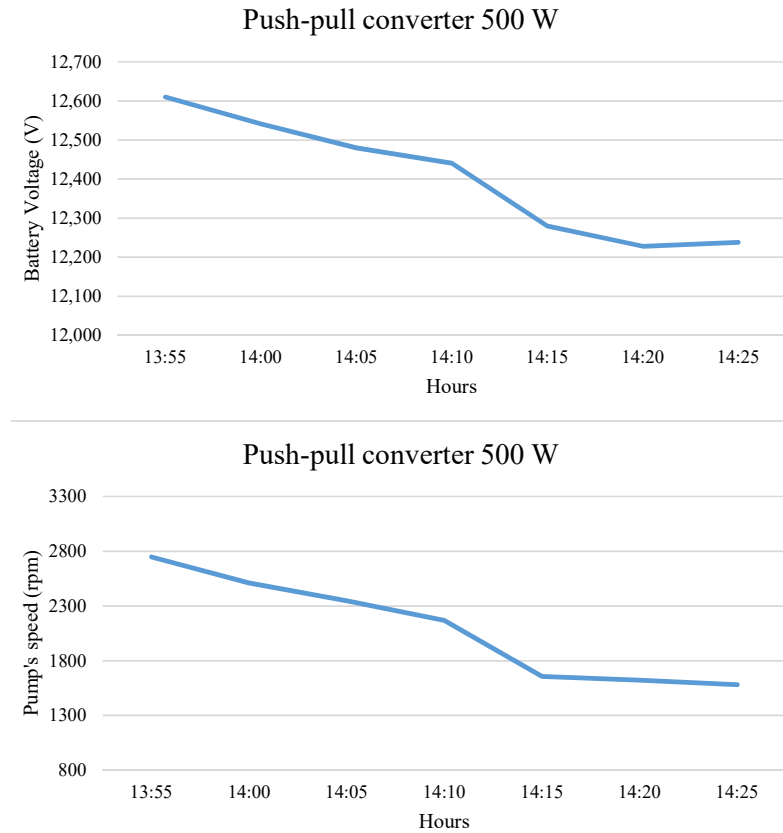
Figure 5.18: V_{bat} and ω_p levels over the afternoon.

Inverter Cotek

Using the data of V_{bat} and ω_p from Table A.4 (Inverter COTEK), the Figure 5.19 was plot. The V_{bat} shows expected results, varying according to the solar irradiance. It decreases linearly because I_{bat-in} is inferior than $I_{bat-out}$. The difference between the values is smaller if compared with results obtained in the test using the battery inverter AJ, but is higher if compared with the push-pull results, as shown in Table A.4. This means that the inverter Cotek requires less current ($I_{bat-out}$) than the battery inverter AJ, and more than the push-pull. The ω_p curve shows expect results, varying according to the V_{bat}.
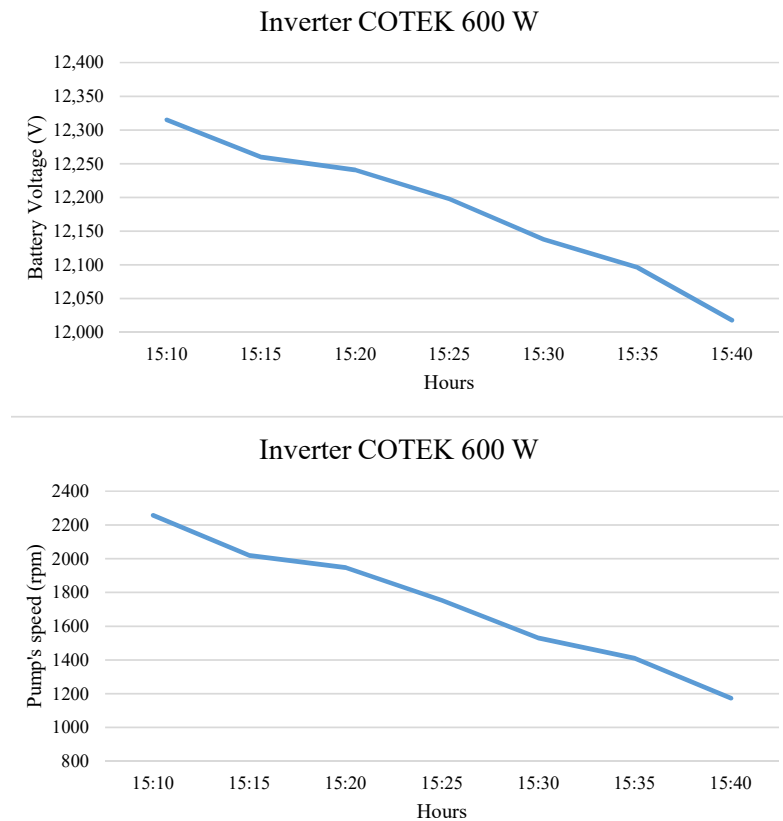
Figure 5.19: V_{bat} and ω_p levels over the afternoon.

5.3 Discussion of the battery design

The results from Test D (section 5.2.4), demonstrated that the difference between $I_{bat-out}$ and I_{bat-in} interfere in the system operation. Furthermore, depending on the battery's state of charge, V_{bat} does not represents at every instant the irradiance variation during the day, because the charge controller's algorithm imposes the output voltage of V_{bat} trying to charge the battery.

Thus, there are two alternatives: a) use two PV modules in parallel to increase I_{pv}, decreasing the difference between $I_{bat-out}$ and $I_{bat-out}$, and stabilize the system operation; or, b) use two batteries of 12 V in series, aiming to halve $I_{bat-out}$. Moreover, considering that in some situations V_{bat} does not represents the irradiance variation during the day, for future works, it is proposed the use of I_{pv}, as reference value to control the ω_p .

Chapter 6

Conclusions and Future Work

The conclusions and future work, on the scope of development of new strategies for PVWPS based on standard components, are presented in this chapter.

6.1 Conclusions

Most of the PVWPS available in the market, are based on dedicated components. Indeed small companies, e.g., J.G. and Valled, are not able to develop their own solutions. Nevertheless for power levels over 1.5 kW, it is possible to design solutions based on the integration of standard components, such as direct connect Photovoltaic (PV) modules to standard frequency converters (SFC), as described in chapter 3. During meetings with the companies cited above, it was verified that there is demand for low power systems, which only one or two PV modules can meet the required power. However, for these systems, the strategy described in chapter 3 results in an over sized PV power, due to the required SFC's input voltage level. Thus, a new approach for low power applications, based on standard components was proposed.

This approach used one/two PV modules, a small battery with charge controller, a DC/AC power module (push-pull), a standard frequency converter SFC (ACS355), and a surface AC pump were used.

A control strategy was implemented in order to control the pump's speed according to the battery voltage level (solar irradiance level). Furthermore, the Depth of Discharge (DOD), was limited to 20% to improve the battery lifetime (number of cycles).

The implemented control method showed promising results. It was verified with real test conditions that the pump's speed vary according to the battery voltage level (irradiance), and DOD was limited to 20% (the system stops if DOD is under this level).

Thus, the objectives of the work were reached. A new approach to PVWPS, for low power applications, was proposed and validated with laboratory tests. This strategy can enable small companies to develop their own solution, based on the integration of standard components, which are widely available in the market, presents high reliability and ruggedness.

6.2 Future Work

In the scope of this project, the potential future works are:

- Continue the JG/Valled challenge using a single phase input output inverter.

- Analysis of different battery inverters and DC/AC power modules.

- Analysis of the more suitable battery storage capacity, and characterization of energy storage in battery *versus* water in tank.

- Analysis of others standard frequency converter (SFC) with single-phase input and output.

- Analysis of others battery charge controller.

- Comparative price analysis between market solutions *versus* standard components.

Bibliography

[1] W. H. Organization, *Use of basic and safely managed drinking water services*, `http://www.who.int/gho/mdg/environmental_sustainability/water/en/`, Oct. 2018.

[2] T. Guardian, *Access to drinking water around the world -in five infographics*, `https://www.theguardian.com/global-development-professionals-network/2017/mar/17/access-to-drinking-water-world-six-infographics`, Mar. 2017.

[3] G. Li, Y. Jin, M. Akram, and X. Chen, "Research and current status of the solar photovoltaic water pumping system – a review", *Renewable and Sustainable Energy Reviews*, vol. 79, pp. 440–458, 2017, ISSN: 1364-0321. DOI: `https://doi.org/10.1016/j.rser.2017.05.055`. [Online]. Available: `http://www.sciencedirect.com/science/article/pii/S1364032117306925`.

[4] S. Chandel, M. N. Naik, and R. Chandel, "Review of solar photovoltaic water pumping system technology for irrigation and community drinking water supplies", *Renewable and Sustainable Energy Reviews*, vol. 49, pp. 1084–1099, 2015, ISSN: 1364-0321. DOI: `https://doi.org/10.1016/j.rser.2015.04.083`. [Online]. Available: `http://www.sciencedirect.com/science/article/pii/S1364032115003536`.

[5] B. Tangerino, D. Roman, V. Leite, A. Goedtel, A. Ferreira, J. Batista, and W. Maidana, "Photovoltaic water pumping system for low power conventional ac pumps", *I Congreso Iberoamericano de Ciudades Inteligentes (ICSC-CITIES 2018)*, Sep. 2018.

[6] A. Barhdadi, "Photovoltaic water pumping systems in rural areas", *4th International Conference on Water Resources and Arid Environments (ICWRAE 4)*, pp. 836–843, Dec. 2010.

[7] V. C. Sontake and V. R. Kalamkar, "Solar photovoltaic water pumping system - a comprehensive review", *Renewable and Sustainable Energy Reviews*, vol. 59, pp. 1038–1067, 2016, ISSN: 1364-0321. DOI: `https://doi.org/10.1016/j.rser.2016.01.021`. [Online]. Available: `http://www.sciencedirect.com/science/article/pii/S1364032116000514`.

[8] M. Bortolini, M. Gamberi, and A. Graziani, "Technical and economic design of photovoltaic and battery energy storage system", *Energy Conversion and Management*, vol. 86, pp. 81–92, 2014, ISSN: 0196-8904. DOI: `https://doi.org/10.1016/j.enconman.2014.04.089`. [Online]. Available: `http://www.sciencedirect.com/science/article/pii/S0196890414004014`.

[9] I. E. Agency, *World energy outlook 2017 - executive summary*, `https://www.iea.org/weo2017/`, Nov. 2017.

[10] S. Europe, *Global market outlook for solar power 2017-2021*, `http://solarpowereurope.org/reports/global-market-outlook-2017`, Jun. 2017.

[11] U. D. of Energy - Office of Indian Energy, *Levelized cost of energy (lcoe)*, `https://energy.gov/sites/prod/files/2015/08/f25/LCOE.pdf`, Aug. 2015.

[12] U. investment Bank Lazard Capital, *Levelized cost of energy 2017*, `https://www.lazard.com/perspective/levelized-cost-of-energy-2017/`, Nov. 2017.

[13] E. Mahmoud and H. el Nather, "Renewable energy and sustainable developments in egypt: Photovoltaic water pumping in remote areas", *Applied Energy*, vol. 74, no. 1, pp. 141–147, 2003.

[14] V. Badescu, "Time dependent model of a complex pv water pumping system", *Renewable Energy*, vol. 28, no. 4, pp. 543–560, 2003, ISSN: 0960-1481. DOI: `https://doi.org/10.1016/S0960-1481(02)00069-1`.

[15] P. Periasamy, N. Jain, and I. Singh, "A review on development of photovoltaic water pumping system", *Renewable and Sustainable Energy Reviews*, vol. 43, pp. 918–925, 2015, ISSN: 1364-0321. DOI: `https://doi.org/10.1016/j.rser.2014.11.019`.

[16] M. Miladi, A. B. Abdelghani-Bennani, I. Slama-Belkhodja, and H. M'Saad, "Improved low cost induction motor control for stand alone solar pumping", in *2014 International Conference on Electrical Sciences and Technologies in Maghreb (CISTEM)*, Nov. 2014, pp. 1–8. DOI: `10.1109/CISTEM.2014.7076955`.

[17] M. Alonso Abella, E. Lorenzo, and F. Chenlo, "Pv water pumping systems based on standard frequency converters", *Progress in Photovoltaics: Research and Applications*, vol. 11, no. 3, pp. 179–191, DOI: `10.1002/pip.475`.

[18] J. Fernández-Ramos, L. Narvarte-Fernández, and F. Poza-Saura, "Improvement of photovoltaic pumping systems based on standard frequency converters by means of programmable logic controllers", *Solar Energy*, vol. 84, no. 1, pp. 101–109, 2010, ISSN: 0038-092X. DOI: `https://doi.org/10.1016/j.solener.2009.10.013`.

[19] A. U. Brito and R. Zilles, "Systematized procedure for parameter characterization of a variable-speed drive used in photovoltaic pumping applications", *Progress in Photovoltaics: Research and Applications*, vol. 14, no. 3, pp. 249–260, DOI: `10.1002/pip.666`.

[20] Y. H. Lim and D. C. Hamill, "Simple maximum power point tracker for photovoltaic arrays", *Electronics Letters*, vol. 36, no. 11, pp. 997–999, May 2000, ISSN: 0013-5194. DOI: `10.1049/el:20000730`.

[21] D. Fiaschi, R. Graniglia, and G. Manfrida, "Improving the effectiveness of solar pumping systems by using modular centrifugal pumps with variable rotational speed", *Solar Energy*, vol. 79, no. 3, pp. 234–244, 2005.

[22] P. Equipments, *Diaphragm and screw pumps*, `https://pumps-pumpingequipments.blogspot.com/2016/11/diaphragm-screw-pump.html`, Nov. 2016.

[23] W. Maidana, V. Leite, A. Ferreira, L. Queijo, J. Batista, J. Bonaldo, and E. Goncalves, "Design of a self-sustainable system based on renewable energy sources for a small museum of science dissemination - the house of silk", *III CONGRESSO IBERO-AMERICANO DE EMPREENDEDORISMO, ENERGIA, AMBIENTE E TEC-NOLOGIA - CIEEMAT 2017*, Jul. 2017.

[24] Ultracell, *Ucg 12-20, specifications*, `http://ultracell.co.uk/products/ucg-batteries/12v`, Oct. 2018.

[25] A. machinery drives, *User's manual, acs355 drives*, `https://library.e.abb.com/public/.../EN_ACS355_UM_D.pdf`, Oct. 2018.

Appendix A

Operation data from tests A, B, C and D

Table A.1: System operation data - Test A.

Hour	Irradiance (W/m²)	Temperature (°C)	I_{pv} (A)	V_{bat} (V)	V_{DC} (V)	V_{Ref} (V)	ω_{pump} (rpm)	I_p (A)
10:35	795,273	16,985	6,4	12,349	215,29	8,288	1091	1,4
10:45	815,571	18,173	6,8	12,346	215,21	8,287	1087	1,4
10:55	833,556	19,574	7,2	12,346	215,22	8,287	1090	1,4
11:05	850,364	18,612	7,5	12,352	215,25	8,291	1105	1,4
11:15	862,111	19,130	7,7	12,359	215,35	8,297	1112	1,4
11:25	877,455	19,912	8,1	12,375	215,62	8,308	1136	1,4
11:35	887,818	19,803	8,2	12,391	215,77	8,317	1155	1,4
11:45	894,889	19,541	8,6	12,417	216,13	8,334	1185	1,4
11:55	909,500	20,722	8,8	12,445	216,53	8,353	1220	1,4
12:05	914,083	21,263	9,0	12,474	216,87	8,371	1252	1,4
12:15	918,417	20,372	9,2	12,508	217,27	8,395	1302	1,4
12:25	926,714	21,544	9,4	12,545	217,65	8,419	1342	1,4
12:35	929,818	21,330	9,5	12,571	217,80	8,438	1384	1,4
12:45	931,308	20,838	9,6	12,598	218,17	8,458	1420	1,4
12:55	937,308	22,561	9,7	12,614	218,35	8,469	1435	1,4
13:05	936,000	22,239	9,6	12,635	218,16	8,482	1467	1,4
13:15	923,583	22,930	9,7	12,634	218,11	8,485	1475	1,4
13:25	615,000	22,653	9,4	12,647	218,25	8,491	1480	1,4
13:35	915,125	23,243	9,3	12,653	218,39	8,492	1477	1,4
13:45	937,750	22,830	9,1	12,650	218,31	8,489	1475	1,4
13:55	927,818	22,730	9,0	12,646	218,30	8,487	1472	1,4
14:05	920,300	22,150	9,0	12,634	218,09	8,479	1460	1,4
14:15	924,300	23,700	8,8	12,609	217,88	8,463	1429	1,4
14:25	912,667	25,888	8,6	12,596	217,88	8,454	1416	1,4
14:35	908,300	26,510	8,6	12,576	217,46	8,437	1384	1,4
14:45	901,000	27,340	8,4	12,555	217,38	8,423	1360	1,4
14:55	890,556	27,497	8,2	12,525	216,89	8,404	1318	1,4
15:05	877,667	27,863	8,2	12,504	216,74	8,389	1297	1,4
15:15	878,700	29,020	8,0	12,476	216,33	8,370	1255	1,4
15:25	855,333	28,863	7,8	12,447	216,08	8,350	1215	1,4
15:35	844,250	27,863	7,5	12,425	215,79	8,335	1201	1,4
15:45	841,900	28,750	7,4	12,406	215,55	8,321	1160	1,4
15:55	819,000	28,418	7,1	12,375	215,02	8,300	1127	1,4
16:05	795,818	28,121	6,9	12,347	214,72	8,282	1091	1,4
16:15	770,571	29,716	6,6	12,327	214,43	8,267	1060	1,4

Table A.2: System operation data - Test B.

Hour	Irradiance (W/m²)	Temperature (°C)	I_{pv} (A)	V_{bat} (V)	V_{DC} (V)	V_{Ref} (V)	ω_{pump} (rpm)	I_p (A)
10:35	838,778	19,797	5,8	12,394	251	8,234	1512	1,4
10:45	860,818	21,521	6,2	12,350	255	8,202	1375	1,4
10:55	869,636	21,003	6,5	12,290	255	8,165	1243	1,4
11:05	877,667	22,463	6,8	12,265	256	8,139	1130	1,4
11:15	893,364	21,139	7,1	12,233	257	8,120	1035	1,4
11:25	901,111	21,286	7,4	12,290	257	8,146	1150	1,4
11:35	906,600	21,910	7,7	12,230	257	8,109	1021	1,4
11:45	910,091	23,985	8,1	12,340	254	8,166	1210	1,4
11:55	914,091	24,694	8,3	12,241	257	8,108	1003	1,4
12:05	918,636	21,448	8,6	12,254	257	8,113	1030	1,4
12:15	925,000	21,303	8,6	12,343	254	8,163	1240	1,4
12:25	929,500	23,850	8,7	12,270	256	8,119	1060	1,4
12:35	933,000	23,752	9,0	12,294	256	8,130	1110	1,4
12:45	936,182	26,094	9,1	12,262	257	8,110	1009	1,4
12:55	932,444	25,119	9,4	12,274	257	8,111	1025	1,4
13:05	160,000	21,412	9,4	12,385	254	8,178	1310	1,4
13:15	524,700	21,390	9,5	12,280	256	8,120	1037	1,4
13:25	553,818	22,403	9,4	12,276	257	8,110	1025	1,4
13:35	964,200	24,510	9,2	12,280	256	8,111	1034	1,4
13:45	938,200	22,860	9,2	12,291	257	8,096	1015	1,4
13:55	930,100	22,290	9,2	12,350	255	8,130	1096	1,4
14:05	909,455	21,857	9,0	12,366	254	8,147	1187	1,4
14:15	936,667	24,319	9,3	12,337	256	8,125	1067	1,4
14:25	919,300	23,130	9,1	12,290	257	8,107	1009	1,4
14:35	709,727	23,130	8,0	12,206	257	8,113	1049	1,4
14:45	695,800	24,890	6,8	12,246	257	8,102	1011	1,4
14:55	791,300	24,150	7,6	12,324	256	8,147	1090	1,4
15:05	765,900	24,800	7,2	12,275	257	8,110	1016	1,4
15:15	889,500	28,172	9,3	12,302	257	8,115	1043	1,4
15:25	719,100	28,890	9,0	12,315	256	8,127	1043	1,4
15:35	681,222	22,619	7,6	12,291	256	8,120	1072	1,4

Table A.3: System operation data - Test C.

Hour	Irradiance (W/m²)	Temperature (°C)	I_{pv} (A)	V_{bat} (V)	V_{DC} (V)	V_{Ref} (V)	ω_{pump} (rpm)	I_p (A)
14:45	624,273	23,085	12,8	12,313	244	8,364	2120	1,4
14:55	795,615	25,615	17,2	12,522	227	8,514	2733	0,9
15:05	756,900	25,260	15,8	12,527	226	8,511	2701	0,9
15:15	716,154	24,868	15,1	12,519	226	8,511	2669	0,9
15:25	685,909	24,612	15,3	13,300	260	9,085	2781	0,9
15:35	651,167	26,647	14,7	12,616	241	8,458	2418	1,1
15:45	604,615	25,707	13,0	12,331	238	8,363	2098	1,4
15:55	557,833	24,788	11,5	12,299	241	8,326	1933	1,4
16:05	496,833	23,830	7,5	12,170	248	8,225	1521	1,4
16:15	431,000	22,713	3,1	12,020	255	8,125	1081	1,4

Table A.4: System operation data - Test D.

Battery Inverter AJ 240 VA									
Hour	Irradiance (W/m²)	I_{pv} (A)	V_{bat} (V)	V_{DC} (V)	V_{Ref} (V)	ω_{pump} (rpm)	I_p (A)	I_{bat-in} (A)	$I_{bat-out}$ (A)
13:10	249,0	2,9	12,148	248	8,289	1730	1,4	3,25	21,1
13:15	504,4	10,8	12,268	243	8,341	1973	1,4	10,4	22,39
13:20	950,0	9,8	12,225	244	8,301	1851	1,4	9,7	21,58
13:25	695,9	3,1	12,036	252	8,178	1302	1,4	3,6	17,83
13:30	858,5	9,5	12,171	248	8,235	1546	1,4	8,9	19,11
13:35	888,0	8,8	12,132	249	8,209	1447	1,4	8,8	18,93
13:40	862,3	8,6	12,202	248	8,256	1585	1,4	8,5	19,11

Push-pull converter 500 W									
Hour	Irradiance (W/m²)	I_{pv} (A)	V_{bat} (V)	V_{DC} (V)	V_{Ref} (V)	ω_{pump} (rpm)	I_p (A)	I_{bat-in} (A)	$I_{bat-out}$ (A)
13:55	863,0	8,3	12,610	211	8,523	2748	0,8	8,2	13,55
14:00	850,3	8,1	12,541	213	8,464	2510	0,8	8,0	11,62
14:05	830,7	7,9	12,480	213	8,418	2347	0,9	7,7	10,68
14:10	835,2	7,7	12,441	213	8,385	2169	1,0	7,7	10,45
14:15	792,1	6,3	12,280	208	8,250	1657	1,4	7,3	10,9
14:20	793,5	6,4	12,228	209	8,263	1623	1,4	7,5	11,04
14:25	797,9	7,6	12,238	208	8,251	1581	1,4	7,5	10,43

Inverter COTEK 600 W									
Hour	Irradiance (W/m²)	I_{pv} (A)	V_{bat} (V)	V_{DC} (V)	V_{Ref} (V)	ω_{pump} (rpm)	I_p (A)	I_{bat-in} (A)	$I_{bat-out}$ (A)
15:10	664,7	8,0	12,315	320	8,408	2257	1,4	7,3	15,87
15:15	653,4	7,6	12,260	322	8,351	2019	1,4	7,2	14,16
15:20	638,8	7,6	12,241	322	8,330	1947	1,4	7,1	13,73
15:25	622,0	7,5	12,198	323	8,286	1753	1,4	7,0	12,66
15:30	584,1	7,1	12,138	323	8,233	1531	1,4	6,6	11,59
15:35	568,9	6,5	12,096	324	8,201	1410	1,4	6,1	11,07
15:40	536,8	4,6	12,018	324	8,148	1174	1,4	4,1	10,09